



Contents lists available at ScienceDirect



Catalysis Today

journal homepage: www.elsevier.com/locate/cattod

Goethite as an efficient heterogeneous Fenton catalyst for the degradation of methyl orange

Yan Wang^{a,b}, Yaowen Gao^a, Lu Chen^a, Hui Zhang^{a,*}

^a Department of Environmental Engineering, Wuhan University, P.O. Box C319, Luoyu Road 129#, Wuhan, 430079, China

^b Department of Environmental Science and Engineering, Anhui Science and Technology University, Donghua Road 9#, Fengyang, 233100, China

ARTICLE INFO

Article history:

Received 13 July 2014

Received in revised form 6 January 2015

Accepted 7 January 2015

Available online xxx

Keywords:

Goethite

Decolorization

Acute toxicity

Heterogeneous Fenton-like catalyst

ABSTRACT

The heterogeneous Fenton process was employed to degrade methyl orange (MO) using goethite as the catalyst. The catalyst stability was evaluated by measuring color removal in three successive cycles. The goethite samples before and after the reaction were characterized by XRD, SEM and FTIR techniques. The effect of major parameters, including pH, H₂O₂ concentration, catalyst addition and initial dye concentration on the decolorization of MO was investigated. The results indicated that the MO decolorization rate increased with the increase of H₂O₂ concentration and catalyst addition, but decreased with the increase of initial MO concentration. The optimal initial pH for the decolorization was found as 3. The acute toxicity experiments illustrated that the *Daphnia magna* mortality declined with the progress of the oxidation.

© 2015 Elsevier B.V. All rights reserved.

1. Introduction

Recently, there has been an increasing concern about color effluents coming from different textile industries and other related industries [1,2], in which approximately different 100,000 types of synthetic dyes are used commonly and 700,000 tons of synthetic dyes are produced annually [1,3,4]. Large amounts of wastewater were generated during the production and utilization process of these dyes [1,3]. Their presence obstructs light penetration and oxygen transfer into water bodies [4]. Among these dyes, azo dyes, characterized by nitrogen-to-nitrogen double-bonds (—N=N—), contribute to more than 50% of the world production of dyes [5]. Methyl orange (MO) is a representative azo dye which is widely used for colorization in textile, paper and chemical industries [6–9]. Due to their toxicity and carcinogenicity, MO and its degradation products threaten to human health and aquatic life safety [9,10]. Therefore, the treatment of MO effluents has attracted the increasing attention [2,6–8]. Unfortunately, MO cannot be effectively destructed by traditional biological methods on account of its bio-recalcitrant and toxic properties [2,11–13]. Although MO could be removed from wastewater by physical processes such as flocculation/coagulation [14,15] and adsorption [16–19], it was just transferred from one phase to another phase, which required further treatment and disposal [2,3,5,20].

Therefore, the effective methods for MO wastewater treatment are required. Nowadays, more and more attention has been paid to the use of advanced oxidation processes (AOPs) in the treatment of dye wastewater [13,21–23]. AOPs can generate hydroxyl radicals ('OH, E⁰ = 2.80 V/SHE), which can oxidize organic pollutants to easily biodegradable small molecules or even carbon dioxide, water and inorganic salts [5,24]. Among the different AOPs, Fenton oxidation process is considered as a promising and potential alternative due to its high efficiency, simple operation and ability to destruct a large range of hazardous organics [11,25]. However, the application of classic Fenton process has been limited by its disadvantages, such as tight pH range and large amount of iron sludge produced [2,5,11,23,25–27].

To overcome these drawbacks, the heterogeneous Fenton process was proposed for the degradation of MO using various catalysts, including Fe₂O₃–SiO₂ [2], H₃PW₁₂O₄₀ supported Fe-bentonite [28], NdFeB magnetic activated carbon [29], and magnetic Fe₂Mo₄ activated carbons [30].

Goethite is one of the most thermodynamically stable iron oxide and formed close-packed array of O²⁻ and OH⁻ anions with Fe³⁺ [31]. As an effective catalyst, it plays a crucial important role in the heterogeneous Fenton processes due to its ubiquity, high catalytic activity, wide range of operating pH, controllable leaching of iron into the solution, large surface area and high surface hydroxyl content [23,31,32]. Both of natural goethite and synthetic goethite have been employed for the treatment of various contaminants, such as C.I. Acid Orange 7, Orange G, PCB28, 2-chlorophenol, benzenesulfonic acid, and so on [13,22,23,31–37]. However, there

* Corresponding author. Tel.: +86 27 68775837; fax: +86 27 68778893.

E-mail address: eeng@whu.edu.cn (H. Zhang).

was little report on the degradation of MO by heterogeneous Fenton process using goethite as catalyst [13]. It was reported that the daughter compounds generated during AOPs might be more toxic compared with their parent compound [35,38,39]. Herein, it is necessary to identify the intermediate products and monitor the change of the toxicity during the degradation of MO by heterogeneous Fenton process. In this study, the goethite was prepared as heterogeneous Fenton catalyst. The effects of various conditions on the decolorization efficiency were investigated. The fresh and used catalysts were characterized by X-ray diffraction (XRD), scanning electron microscope (SEM) and Fourier transform infrared spectrometer (FTIR). The changes of TOC and acute toxicity were monitored.

2. Experiment

2.1. Materials

Methyl orange was purchased from Shanghai Shiyi Chemicals Reagent Co. Ltd. (China) and used as received. Hydrogen peroxide (analytical grade, 30%, w/w) was obtained from Shanghai Sinopharm Chemical Reagent Co., Ltd. H_2SO_4 and NaOH were obtained from Chengdu Institute of the Joint Chemical Reagent (China) and used as received. All solutions were prepared with deionized water.

2.2. Preparation and characterization of the catalyst

Goethite was prepared based on our previous study [23]. The morphology of the catalyst was carried out using a scanning electron microscope (SEM, Zeiss EVO LS-185, UK) operated at 20.0 kV. X-ray diffraction (XRD) patterns were recorded on a D/Max-2550 PC diffractometer in θ - 2θ configuration to identify the crystal phase and structure. The wide angle data were collected from 20° to 90° on 2θ scale, when the operated condition was set at 36 kV/24 mA, using Cu K α 1 radiation with a wavelength of 1.5406 Å.

The infrared spectra of synthesized goethite were recorded on KBr pellets by a Fourier transform infrared spectrometer (FTIR, Nicolet Avatar 330). To avoid moisture uptake, KBr pellets were prepared by pressing mixtures of dry powdered sample and spectrometry-grade KBr under vacuum. One hundred and fifty scans were collected for each sample in the range of 400–4000 cm⁻¹ with a resolution of 2 cm⁻¹.

2.3. Procedure

In all experiments, a stock solution of MO was prepared fresh before each run and the initial concentration (C_0) was kept at 75 mg L⁻¹. The solution pH was measured with a Mettler Toledo FE20 pH-meter.

The experiments were performed in a glass beaker containing 200 mL solution at room temperature (20 °C). A given amount of hydrogen peroxide and goethite were added into the reactor. A magnetic stirrer provided complete mixing of the solution in the reactor. At pre-selected time intervals, samples were removed by a syringe and filtered through 0.22 μm membranes before the absorbance was measured.

2.4. Analysis methods

The absorbance of MO was measured at λ_{max} = 464 nm using a Shimadzu UV-1700 spectrophotometer. Total organic carbon (TOC) was analyzed using a TOC analyzer (Shimadzu TOC-L) to evaluate the mineralization of MO. The total iron leached from goethite

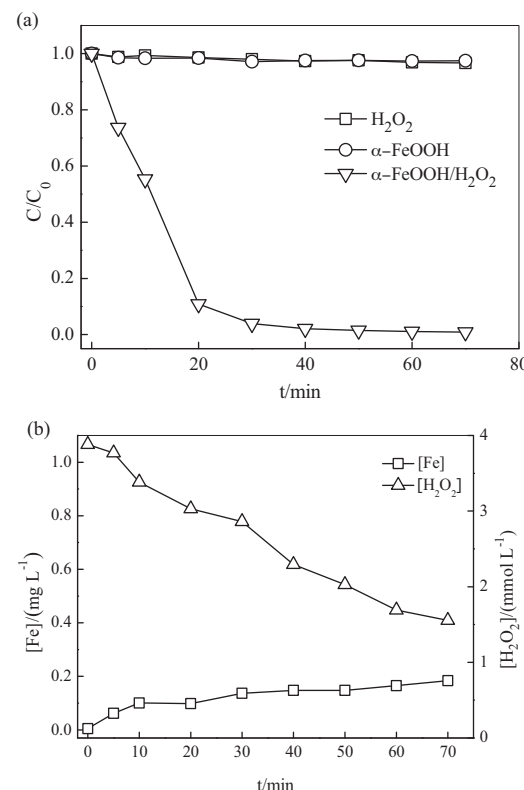


Fig. 1. (a) Degradation of MO under different conditions, (b) H_2O_2 decomposition and the iron leaching with reaction time ($[MO] = 75 \text{ mg L}^{-1}$, $[H_2O_2] = 3.88 \text{ mmol L}^{-1}$, $pH = 3$, $[\text{goethite}] = 0.3 \text{ g L}^{-1}$).

was evaluated by phenanthroline spectrophotometry during catalytic tests [40]. The active toxicity was determined with *Daphnia magna* (*D. magna*) immobilization essays [41]. *D. magna* was cultured in laboratory for more than three generations. The acute toxicity experiments were performed using 25 24-h-old *D. magna* in 50-mL-capacity test beakers which were divided into five groups. Four groups were used for the test while one group for the blank. They were set in the incubator which was set at 20 °C in a 16 h light–8 h dark cycle. No foods were given during the acute toxic test. The number of immobilized *D. magna* was counted after 24 h, and the experiments were repeated five times.

3. Results and discussion

3.1. Decolorization of MO under different systems

To investigate the removal of MO under different conditions, the experiments were carried out with H_2O_2 alone, goethite alone and goethite/ H_2O_2 , respectively.

As presented in Fig. 1(a), the color of MO was hardly removed by either H_2O_2 or goethite alone. It is due to the limited oxidation power of H_2O_2 and the lower adsorption capacity of goethite. When goethite was added with H_2O_2 simultaneously, the decolorization efficiency reached 98.9% within 70 min reaction, and this goethite catalyst showed higher catalytic activity compared with other catalysts [13,29]. For example, Li and Zhang [13] reported that the decolorization efficiency could reach nearly 98% within 80 min reaction when MO was oxidized by heterogeneous Fenton in combination with UV using the amorphous FeOOH catalyst. However, 2.5 g L⁻¹ catalyst and 15.8 mmol L⁻¹ H_2O_2 were required by the oxidation process. Yang et al. [29] also reported that the MO removal efficiency could reach 97.1% by Fenton-like process with

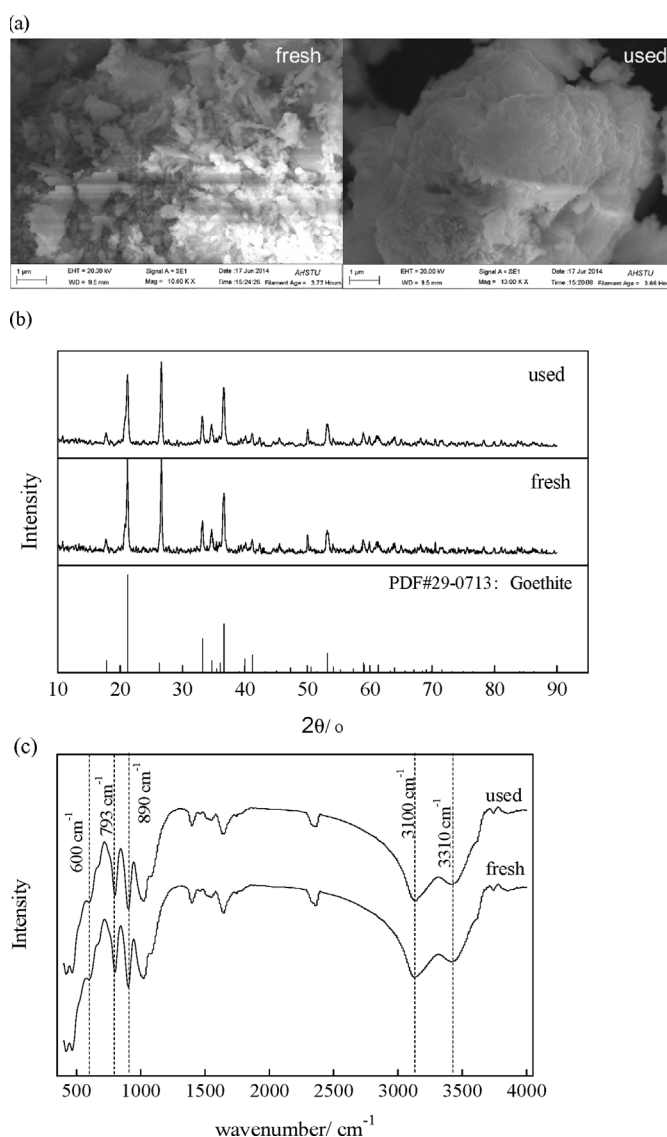


Fig. 2. Characterization of fresh and used goethite: (a) SEM image, (b) XRD pattern, (c) FTIR spectra.

NdFeB magnetic activated carbon catalyst, but the catalyst dosage was as high as 10 g L^{-1} .

It could be known from Fig. 1(b) that H_2O_2 concentration decreased with the increasing reaction time, clearly illustrating that H_2O_2 could be activated by goethite to generate $\cdot\text{OH}$ which further oxidized MO. After 40 min reaction, the bleaching of MO was completed basically, but H_2O_2 still remained and tended to decompose gradually. It could be understood that the complete bleaching did not denote the whole mineralization of MO to CO_2 , H_2O , and so on, and H_2O_2 was still required for further degradation of intermediate products. The iron leaching increased gradually during the oxidation process, but the maximum concentration of the iron leaching was less than 0.2 mg L^{-1} and the homogeneous Fenton reaction could be ignored for the MO degradation.

3.2. Characterization of fresh and used catalyst

The morphology of fresh goethite was observed through SEM images. As illustrated in Fig. 2(a), the sample particles with rough surface and the common acicular structure were observed for fresh catalyst. The XRD analysis was applied to define the structure of fresh goethite and the obtained patterns were shown on Fig. 2(b).

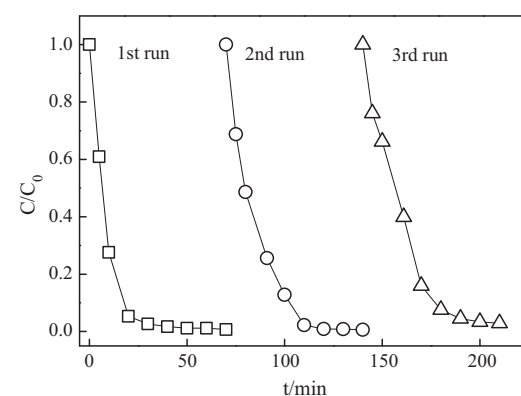


Fig. 3. Reusability of goethite for the decolorization of MO ($[\text{MO}] = 75 \text{ mg L}^{-1}$, $[\text{H}_2\text{O}_2] = 3.88 \text{ mmol L}^{-1}$, pH = 3, [goethite] = 0.3 g L^{-1}).

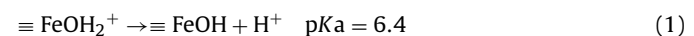
The peaks at the angle 2θ of 21.223° , 33.241° , 34.700° , 36.649° , 39.984° , 41.186° , 50.613° , 53.237° , and 59.023° , are specific of goethite [42,43]. The FTIR spectra of fresh catalyst were shown in Fig. 2(c), and various functional groups represented in the IR spectra were the same as that of goethite. The band between 3000 and 3500 cm^{-1} is generated by the stretching of free/bonded hydroxyl groups [44]. The peaks at about 890 and 793 cm^{-1} are attributed to O–H bending bands in goethite (Fe–OH) and are respectively on behalf of the vibration in and out of the plane [44]. The band absorption at 600 cm^{-1} is assigned to Fe–O stretching vibrations [44,45]. According to the result of the XRD patterns, SEM image and FTIR spectra of the fresh catalyst, the powder synthesized is goethite.

As can be seen in Fig. 2(a), the SEM image of used goethite was obviously different from that of fresh one. For fresh catalyst, lots of the sample particles with rough surface and the common acicular structure were observed. The surface of used catalyst became smooth and the catalyst particles were aggregated in an irregular shape. Despite of this, the surface of agglomerate catalyst still showed the acicular pattern. However, almost no change of the structure was discovered between fresh and used goethite in Fig. 2(b). Moreover, the FTIR spectra of used catalyst were nearly the same as that of fresh catalyst in Fig. 2(c).

In order to further confirm the stability of the goethite catalyst, the reuse experiments were performed. Under the same conditions (75 mg L^{-1} MO, 0.3 g L^{-1} goethite, 3.88 mmol L^{-1} H_2O_2 , and pH 3), the experiments of the catalytic degradation of MO was repeated for three cycles and each experiment was lasted for 70 min. The reused catalyst was filtered and rinsed with deionized water after each repeated experiment, then dried around 100°C . As shown in Fig. 3, 99.3, 99.4 and 97.1% of the MO removal were obtained in three successive cycles, respectively. The decolorization efficiencies of MO are nearly the same in three successive cycles, indicating synthesized goethite is an excellent long-term stable catalyst for the goethite/ H_2O_2 system.

3.3. Effect of major parameters on the MO removal

Experiments under various reaction conditions (pH, H_2O_2 , catalyst addition and initial MO concentration) were conducted and the results were shown in Fig. 4. As can be seen in Fig. 4(a), the decolorization efficiency increased when initial pH was decreased from 7 to 3. The surface functional groups of goethite are influenced by the solution pH according to the following equation [31,46,47]:



The ratio of positively charged $\equiv \text{FeOH}_2^+$ groups increased as pH decreased. The MO is generally negatively charged since the sulfonated group ($-\text{SO}_3^-$) in its structure is hydrolyzed [2]. On account

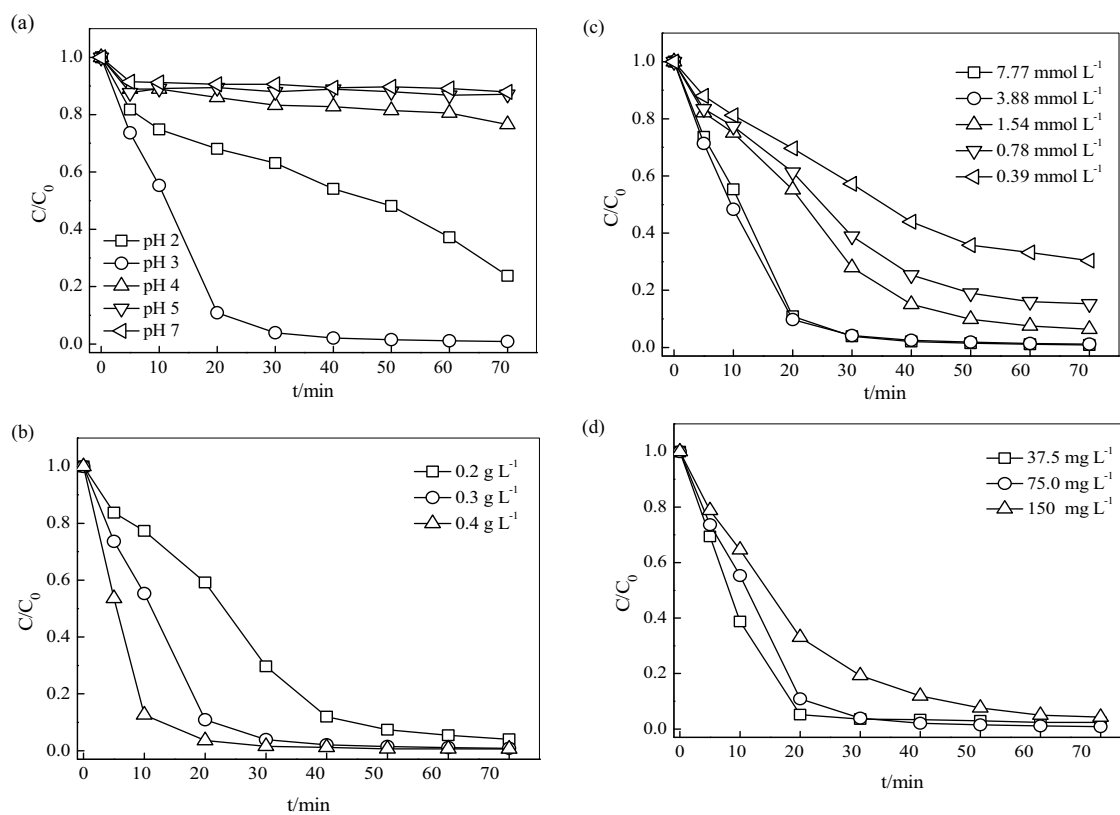


Fig. 4. Effect of major parameters on the MO removal: (a) pH, (b) goethite addition, (c) H_2O_2 concentration and (d) initial MO concentration ($[\text{MO}] = 75 \text{ mg L}^{-1}$, $\text{pH} = 3$, $[\text{H}_2\text{O}_2] = 3.88 \text{ mmol L}^{-1}$, $[\text{goethite}] = 0.3 \text{ g L}^{-1}$).

of the electrostatic attraction, the acidic solution condition favors the adsorption of MO onto the goethite surface [6]. Moreover, the MO prefers the quinoid structure which undergoes oxidation by $\cdot\text{OH}$ more easily than the azo structure at lower initial pH values [2].

Fig. 4(a) illustrated that the decolorization was suppressed as the initial pH was further decreased to 2. When pH value was below 3, H_2O_2 could capture a proton and turn into more stable oxonium ion H_3O_2^+ [48,49],



On the other hand, hydrogen ion would act as the scavenger of hydroxyl radicals at a very low pH [23,46],



where electrons may be gained from ferrous ions. Therefore, the decolorization rate decreased as the pH dropped from 3 to 2.

Fig. 4(b) depicted the decomposition of MO at goethite addition of $0.2 - 0.4 \text{ g L}^{-1}$ when the pH was 3, the MO concentration was 75 mg L^{-1} and the H_2O_2 concentration was 3.88 mmol L^{-1} . As illustrated in Fig. 4(b), the decolorization efficiency of MO significantly increased from 40.8 to 96.4% after 20 min reaction when goethite addition increased from 0.2 to 0.4 g L^{-1} . The decolorization of azo dyes is mainly through heterogeneous Fenton reaction, which depends on active sites in the specific area of the catalyst [20]. The increase of goethite addition corresponds to the increase of the total area, which would result in the faster H_2O_2 decomposition to generate $\cdot\text{OH}$ through the increase of active sites. Thus, the removal rate of organic pollutants is improved with increasing goethite addition [32]. Although the increase of goethite addition resulted in the increase of decolorization rate, the decolorization efficiency after 70 min reaction was nearly the same at the fixed H_2O_2 concentration, which was higher than 96.0% as illustrated

in Fig. 4(b). This is because the amount of generated $\cdot\text{OH}$ was only dependent on H_2O_2 dosage, and 3.88 mmol L^{-1} H_2O_2 was sufficient to generate $\cdot\text{OH}$ when only decolorization was concerned.

In order to achieve the maximum color removal, the effect of the H_2O_2 concentration on the decolorization of MO was investigated when the pH was 3, the MO concentration was 75 mg L^{-1} and goethite addition was 0.3 g L^{-1} . Hydrogen peroxide is a source of hydroxyl radicals in the goethite/ H_2O_2 system, and more $\cdot\text{OH}$ would be generated to oxidize MO at higher H_2O_2 concentration. As shown in Fig. 4(c), the MO removal efficiency increased with an increase in H_2O_2 concentration from 0.39 to 3.88 mmol L^{-1} . However, the further increase in H_2O_2 concentration could not result in an increase of MO removal efficiency. This is due to the fact that the overdosed H_2O_2 would scavenge $\cdot\text{OH}$ at H_2O_2 concentration higher than 3.88 mmol L^{-1} [25,50],



The generated hydroperoxy radicals were less active than hydroxyl radicals and could not improve decolorization efficiency.

The initial dye concentration is usually considered as one of the most important parameters for the dye removal. To elucidate the effect of the initial dye concentration on the decolorization of MO, the initial MO concentrations were set at 37.5 , 75.0 , 150 mg L^{-1} , respectively, when the pH was 3, the H_2O_2 concentration was 3.88 mmol L^{-1} and goethite addition was 0.3 g L^{-1} . As shown in Fig. 4(d), the MO removal efficiency decreased significantly with increasing initial dye concentration. After 20 min reaction, the decolorization efficiency reached 94.8 and 67.0% when the initial MO concentrations were 37.5 and 150 mg L^{-1} , respectively. As the non-selective oxidants, $\cdot\text{OH}$ could oxidize not only target pollutants, but also the intermediates generated during the reaction process. When hydrogen peroxide concentration and amount of goethite are fixed in the goethite/ H_2O_2 system, the amount

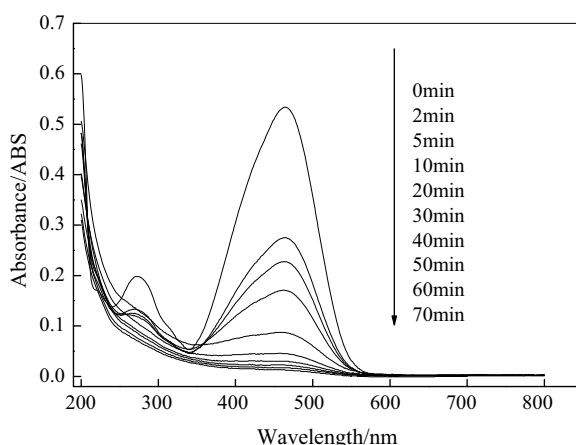


Fig. 5. UV-Vis spectral changes with reaction time ($[MO] = 75 \text{ mg L}^{-1}$, $[H_2O_2] = 3.88 \text{ mmol L}^{-1}$, $pH = 3$, [goethite] = 0.3 g L^{-1}).

of formed $\cdot\text{OH}$ in this process is also constant. However, the probability of reaction between MO molecules and the hydroxyl radicals would be decreased with the increase of initial MO concentration [20]. In addition, more intermediate products would compete with MO for $\cdot\text{OH}$. These resulted in the decline of the MO decolorization rate. Despite of the competitive consumption of hydroxyl radicals, the color was nearly removed completely at different initial dye concentration, indicating hydroxyl radicals generated from the goethite/ H_2O_2 oxidation system were sufficient enough to bleach MO completely after 70 min reaction.

3.4. Analysis of UV-visible spectra changes

To investigate the degradation of MO in the heterogeneous Fenton process, representative UV-Vis spectra changes of MO solution as a function of reaction time were shown in Fig. 5. It can be seen that the absorption spectrum of MO in aqueous solution is mainly characterized by two bands. One main band in the visible region located at 464 nm resulted from an extended chromophore comprising of both aromatic rings, which connected through the azo bond. The other band in the ultraviolet region located at 272 nm was attributed to the $\pi\rightarrow\pi^*$ transition related to aromatic rings in the MO molecule [2,13,51]. As the reaction proceeded, the two characteristic absorption peaks at 272 and 464 nm decreased gradually and essentially disappeared after 70 min. The continuously decrease of the band at 464 nm with the reaction time indicated the azo-band chromophore and conjugated π^* systems were destroyed. Meanwhile, the decline of zone around 272 nm illustrated that the aromatic rings were also decomposed.

3.5. The changes of TOC and acute toxicity with reaction time

As is well known, the complete decolorization of azo dye does not mean that it is completely oxidized to small inorganic molecules and the toxicity disappears. Thus, the mineralization and the acute toxic tests were determined before and after degradation of MO by goethite/ H_2O_2 . As shown in Fig. 6, less than 13% TOC was removed after 10 min reaction compared with 45% MO decolorization efficiency. When the decolorization efficiency of MO nearly reached 100% after 30 min reaction, the TOC removal rate was still less than 40%. When the reaction time was extended to 60 min, 55% of TOC removal efficiency could be achieved.

The evolution of the acute toxicity of the MO degradation effluents for *D. magna* with the reaction time was shown in Fig. 6. As can be seen from Fig. 6, the *D. magna* immobilization rate of the initial MO solution was 100% after 24 h exposition. As the oxidation

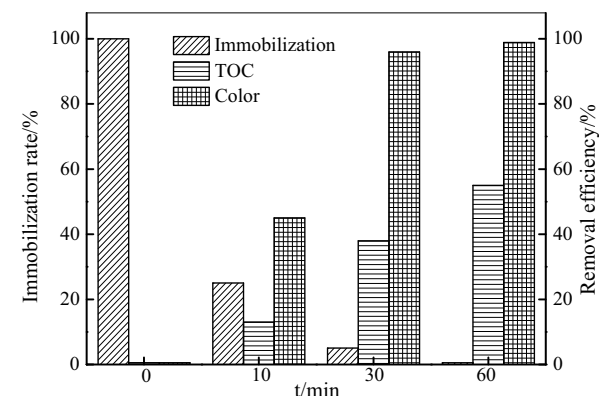


Fig. 6. The mineralization and the changes of active toxicity with reaction time ($[MO] = 75 \text{ mg L}^{-1}$, $[H_2O_2] = 3.88 \text{ mmol L}^{-1}$, $pH = 3$, [goethite] = 0.3 g L^{-1}).

process proceeded, the acute toxicity gradually decreased compared with the initial MO solution, indicating the toxic structures of MO and the immediate products were degraded into the less toxic products.

4. Conclusions

The results obtained from this work indicate that goethite is an efficient catalyst for the degradation of MO by heterogeneous Fenton. The decolorization was mainly attributed by the heterogeneous Fenton reaction and the homogeneous Fenton reaction could be ignored. The degradation rate of MO is improved with the increase of goethite addition and H_2O_2 concentration but decreased with increasing of initial MO concentration. Recycle experiments showed goethite was stable and can be reused. As clearly proved by UV-Vis changes with the reaction time, MO quickly reacted with free radical to form by-products. Toxicity to *D. magna* decreased gradually with reaction time. Therefore, the goethite/ H_2O_2 system is a promising process for the treatment of dye wastewater.

Acknowledgment

This study was supported by National Natural Science Foundation of China (Grant No. 20977069).

References

- [1] L. Guz, G. Curutchet, R.M. Torres Sánchez, R. Candal, J. Environ. Chem. Eng. 2 (2014) 2344–2351.
- [2] N. Panda, H. Sahoo, S. Mohapatra, J. Hazard. Mater. 185 (2011) 359–365.
- [3] M.L. Rache, A.R. García, H.R. Zea, A.M.T. Silva, Appl. Catal. B: Environ. 146 (2014) 192–200.
- [4] M. Siddique, R. Farooq, G.J. Price, Ultrason. Sonochem. 21 (2014) 1206–1212.
- [5] H. Lin, H. Zhang, X. Wang, L.G. Wang, J. Wu, Sep. Purif. Technol. 122 (2014) 533–540.
- [6] J. Fan, Y.H. Guo, J.J. Wang, M.H. Fan, J. Hazard. Mater. 166 (2009) 904–910.
- [7] W.Y. He, Q.L. Ma, J. Wang, J. Yu, W.R. Bao, H.Z. Ma, Appl. Clay Sci. 99 (2014) 178–186.
- [8] Z.H. Xu, J.R. Liang, L.X. Zhou, J. Alloys Compd. 546 (2013) 112–118.
- [9] A. Mittal, A. Malviya, D. Kaur, J. Mittal, L. Kurup, J. Hazard. Mater. 148 (2007) 229–240.
- [10] X.H. Zhao, Y.P. Lu, D.R. Phillips, H. Hwang, I.R. Hardin, J. Chromatogr. A 1159 (2007) 217–224.
- [11] L.G. Devi, S.G. Kumar, K.M. Reddy, C. Munikrishnappa, J. Hazard. Mater. 164 (2009) 459–467.
- [12] M.M. El-Sheekh, M.M. Gharieb, G.W. Abou-El-Soud, Int. Biodeterior. Biodegrad. 63 (2009) 699–704.
- [13] Y. Li, F.S. Zhang, Chem. Eng. J. 158 (2010) 148–153.
- [14] Z. Yang, H. Yang, Z.W. Jiang, T. Cai, H.J. Li, H.B. Li, A.M. Li, R.S. Cheng, J. Hazard. Mater. 254–255 (2013) 36–45.
- [15] K.W. Pi, Q. Xiao, H.Q. Zhang, M. Xia, A.R. Gerson, Process Saf. Environ. Prot. 92 (2014) 796–806.
- [16] T. Kou, Y.Z. Wang, C. Zhang, J.Z. Sun, Z.H. Zhang, Chem. Eng. J. 223 (2013) 76–83.
- [17] S. Hosseini, M.A. Khan, M.R. Malekbala, W. Cheah, T.S.Y. Choong, Chem. Eng. J. 171 (2011) 1124–1131.

- [18] J. Goscianska, M. Marcinia, R. Pietrzak, *Chem. Eng. J.* 247 (2014) 258–264.
- [19] J.S. Liu, S. Ma, L.J. Zang, *Appl. Surf. Sci.* 265 (2013) 393–398.
- [20] H. Zhang, F. Liu, X.G. Wu, J.H. Zhang, D.B. Zhang, *Asia-Pac. J. Chem. Eng.* 4 (2009) 568–573.
- [21] H.Y. Xu, T.N. Shi, L.C. Wu, S.Y. Qi, *Water Air Soil Pollut.* 224 (2013) 1740–1750.
- [22] Y.J. Shih, C.H. Ho, Y.H. Huang, *Water Environ. Res.* 85 (2013) 340–345.
- [23] H. Zhang, H. Fu, D.B. Zhang, *J. Hazard. Mater.* 172 (2009) 654–660.
- [24] H.B. Hadjiltaief, P. Da Costa, P. Beaunier, M.E. Gálvez, *Appl. Clay Sci.* 91–92 (2014) 46–54.
- [25] K. Rusevova, R. Köferstein, M. Rosell, H.H. Richnow, F.D. Kopinke, A. Georgi, *Chem. Eng. J.* 239 (2014) 322–331.
- [26] X.Y. Zhang, Y.B. Ding, H.Q. Tang, X.Y. Han, *Chem. Eng. J.* 236 (2014) 251–262.
- [27] H. Zhang, D.B. Zhang, J.Y. Zhou, *J. Hazard. Mater. B* 135 (2006) 106–111.
- [28] G.T. Wei, C.Y. Fan, L.Y. Zhang, R.C. Ye, T.Y. Wei, Z.F. Tong, *Catal. Commun.* 17 (2012) 184–188.
- [29] C.W. Yang, D. Wang, Q. Tang, *J. Taiwan Inst. Chem. Eng.* 45 (2014) 2584–2589.
- [30] T.D. Nguyen, N.H. Phan, M.H. Do, K.T. Ngo, *J. Hazard. Mater.* 185 (2011) 653–661.
- [31] H.B. Liu, T.H. Chen, R.L. Frost, *Chemosphere* 103 (2014) 1–11.
- [32] Z.R. Lin, X.H. Ma, L. Zhao, Y.H. Dong, *Chemosphere* 101 (2014) 15–20.
- [33] J. He, W.H. Ma, W.J. Song, J.C. Zhao, X.H. Qian, S.B. Zhang, J.C. Yu, *Water Res.* 39 (2005) 119–128.
- [34] G.B. Ortiz de la Plata, O.M. Alfano, A.E. Cassano, *Appl. Catal. B: Environ.* 95 (2010) 1–13.
- [35] Y. Wang, H. Zhang, L. Chen, *Catal. Today* 175 (2011) 283–292.
- [36] G.B. Ortiz de la Plata, O.M. Alfano, A.E. Cassano, *J. Photochem. Photobiol. A: Chem.* 233 (2012) 53–59.
- [37] J.J. Wu, M. Muruganandham, J.S. Yang, S.S. Lin, *Catal. Commun.* 7 (2006) 901–906.
- [38] A. Karci, *Chemosphere* 99 (2014) 1–18.
- [39] T. Olmez-Hancı, D. Dursun, E. Aydin, I. Arslan-Alaton, B. Girit, L. Mita, N. Diano, D.G. Mita, M. Guida, *Chemosphere* 119 (2015) S115–S123.
- [40] Z.O. Tesfalidet, J.F.V. Staden, R.I. Stefan, *Talanta* 64 (2004) 1189–1195.
- [41] Organization for Economic Cooperation and Development (OECD), *Daphnia sp. Acute Immobilization Test. Test Guideline No. 202, OECD Guidelines for Testing of Chemicals*, 2004.
- [42] A. Jaiswal, S. Banerjee, R. Mani, M.C. Chattopadhyaya, *J. Environ. Chem. Eng.* 1 (2013) 281–289.
- [43] J.S. Markovski, V. Đokić, M. Milosavljević, M. Mitrić, *Ultrason. Sonochem.* 21 (2014) 790–801.
- [44] L.C.A. Oliveira, T.C. Ramalho, E.F. Souza, M. Gonçalves, D.Q.L. Oliveira, M.C. Pereira, J.D. Fabris, *Appl. Catal. B: Environ.* 83 (2008) 169–176.
- [45] N. Sankararamakrishnan, A. Gupta, S.R. Vidyarthi, *J. Environ. Chem. Eng.* 2 (2014) 802–810.
- [46] T. Zhang, C.J. Li, J. Ma, H. Tian, Z.M. Qiang, *Appl. Catal. B: Environ.* 82 (2008) 131–137.
- [47] M. Muruganandham, J.J. Wu, *Catal. Commun.* 8 (2007) 668–672.
- [48] B.G. Kwon, D.S. Lee, N. Kang, H.Y. Xu, W.C. Liu, J. Shi, H. Zhao, S.Y. Qi, *Water Res.* 33 (1999) 2110–2118.
- [49] M. Zhou, Q. Yu, L. Lei, G. Barton, *Sep. Purif. Technol.* 57 (2007) 380–387.
- [50] J. Wu, H. Zhang, N. Oturan, Y. Wang, L. Chen, M.A. Oturan, *Chemosphere* 87 (2012) 614–620.
- [51] H. Zhang, L.J. Duan, D.B. Zhang, *J. Hazard. Mater.* 138 (2006) 53–59.